

INDUSTRIAL HOT ROLLING OF AN AA3004 ALLOY; EXPERIMENTAL INVESTIGATIONS AND MODELLING OF RECRYSTALLISATION

Hans Erik VATNE*, Anders OSCARSSON** and Hans-Erik EKSTRÖM**

* Hydro Aluminium, R&D Materials Technology, N-6600 Sunndalsøra, Norway

** Gränges Technology, S-61281 Finspång, Sweden

ABSTRACT A model for recrystallisation after hot deformation of aluminium alloys has recently been developed. The model is based on experimental investigations of recrystallisation behaviour and deformed microstructure and texture of hot plane strain compressed AA1050 and AA3104 alloys, where special attention has been paid to the industrially relevant cube orientation. In the present paper the model has been applied to industrial hot rolling. The rolling schedule consisted of 14 passes in a reversible break-down mill followed by a 2-stand tandem mill. The rolling schedule is characterised by decreasing temperatures, increasing driving pressures and increasing inter-pass times with increasing pass number. Modelled fractions recrystallised after each rolling pass, textures and grain sizes were compared to experimental results, although samples from all passes were not available for practical reasons. Both model predictions and experimental data showed the highest fractions of recrystallisation in the final rolling passes, and reasonable model predictions were obtained for recrystallised grain size and cube texture.

Keywords: *Rolling, recrystallisation, cube texture, modelling*

1. INTRODUCTION

Microstructural modelling of recrystallisation is important for several reasons: (i) empirical methods without an understanding of the recrystallisation mechanisms are no longer sufficient for further improvement of product quality and reduction of production costs, (ii) microstructural models give truly predictive capabilities in relation to the effect of process variables on subsequent processing and product properties in contrast to empirical relationships, (iii) industrial tests are expensive and difficult to perform, (iv) laboratory simulations are unable to reproduce all industrial conditions, (v) models are required to handle the complexity of industrial thermo-mechanical processing and (vi) models may help initiate new experiments that will provide a more profound understanding of the mechanisms responsible for the microstructural changes.

Modelling of thermo-mechanical processing is well established as a valuable tool for optimising processing conditions in the steel industry, even for complex processes like rolling. For aluminium, the modelling is more difficult due to a higher complexity and a higher demand on knowledge of the physical mechanisms behind the recrystallisation process in order to obtain satisfactory model predictions. The recrystallisation process during hot rolling of steels can be satisfactorily described in terms of only one microstructural parameter; the initial grain size, in addition to the parameters describing the material and the rolling schedule. It has turned out to be impossible to describe recrystallisation during hot rolling of aluminium properly by an approach similar to that applied for steels [1-2]. In these attempts it has been concluded that the simulated microstructures appear unrealistic and that some important unresolved questions in relation to modelling hot rolling of aluminium exist. It appears that a more sophisticated and fundamental description of the microstructure evolution is required for Al-alloys than for steels. This description has to include a physical characterisation of the potential nucleation sites for recrystallisation and their respective efficiency under various deformation conditions. An approach based on such principles has the additional advantage of predicting the recrystallisation texture evolution.

A physically based model for predicting recrystallisation microstructures and textures after hot deformation of aluminium has recently been developed [3,4]. Notice that the model has been developed for plane strain deformation conditions, and is thus applicable in the central regions of rolled sheets. The model has proved to give very reasonable predictions of single pass hot deformation of aluminium. The present paper aims at handling the more complex situation of multipass deformation, where control of partial recrystallisation between deformation passes becomes an essential feature. The ultimate goal of such an approach is to model an entire industrial hot rolling mill. Attempts to this have already been undertaken [4], but the problem is to validate the model output. In the present paper the model has been applied to industrial hot rolling. The rolling schedule consisted of 14 passes in a reversible break-down mill followed by a 2-stand tandem mill. The rolling schedule is characterised by decreasing temperatures, increasing driving pressures and increasing inter-pass times with increasing pass number. Modelled fractions recrystallised after each rolling pass, textures and grain sizes were compared to experimental results, although samples from all passes were not available for practical reasons.

2. MODEL CONCEPT

The recently developed model for recrystallisation kinetics, textures and grain sizes of hot deformed aluminium alloys (for plane strain deformation conditions) has been described in detail elsewhere [3-4], and will therefore only be briefly outlined here.

It is of vital importance to know the nature of the nucleation sites for recrystallised grains in order to make a successful recrystallisation model. Particle stimulated nucleation (PSN) is known to be an important nucleation mechanism in commercial alloys [5]. The nuclei that are created in the deformation zones around large particles are assumed to have random orientations. The critical particle size, η^* , for a successful nucleation of a grain can be derived by using the familiar Gibbs-Thompson equation, giving $\eta^* = 4\gamma_{GB}/(P_D - P_Z)$, where γ_{GB} is the specific grain boundary energy between the nucleus and the deformation matrix, $(P_D - P_Z)$ is the effective driving pressure for recrystallisation where P_D is the stored energy and P_Z is the retarding force from finely dispersed precipitates. The density of PSN sites, N_{PSN} , is determined by an integration of the particle size distribution $f(\eta)$ which is characterised through the distribution parameters N_0 and L . The density of PSN nuclei becomes:

$$N_{PSN} = C_{PSN} N_0 \exp\left(-\frac{4\gamma_{GB}}{P_D - P_Z}\right) \quad (1)$$

where C_{PSN} is a constant which determines the number of recrystallised grains nucleated at each particle that is larger than η^* .

Investigations of hot deformed aluminium alloys [6-7] have demonstrated that the nucleation of the cube recrystallisation texture component is associated with cube grains that were present in the starting material and remained orientation stable during deformation, by which a cube band capable of regenerating new cube grains has been established. The following observations summarise the basis for this nucleation mechanism: (i) Cube oriented grains are metastable during hot deformation and are deformed to band-like shapes. (ii) Subgrains within the cube bands have a size advantage compared to subgrains of other orientations, where the largest subgrains are potential recrystallisation nuclei upon subsequent annealing. (iii) The existence of a cube-S high angle boundary (i.e. cube band is surrounded by an $S = \{123\} \langle 634 \rangle$ neighbour deformation texture component) promotes nucleation from the cube bands. It follows that the density of cube sites, N_c , is given by $N_c = \delta_c A(\epsilon)(1 - R_c) R_s S_c^*$, where δ_c is the average cube subgrain size (given by the Zener-Hollomon parameter, $Z = \epsilon' \exp[Q/RT]$), $A(\epsilon)$ is the surface area per unit volume of cube grains that have undergone a deformation of an effective strain ϵ , R_s is the fraction of cube bands

surrounded by the S deformation texture component and S_c^* is the density of overcritically large subgrains within the cube bands. $A(\varepsilon)$ is given by the initial cube grain size D_0 and the instantaneous volume fraction of cube in the material, $R_c=f(\varepsilon, Z)$. The density of overcritically large subgrains is determined by a numerical integration of the subgrain size distribution. The density of cube nuclei becomes:

$$N_C = 2C_C (\delta_C/\bar{D})R_C (1 - R_C)R_S S_C^* [\exp(\varepsilon) + \exp(-\varepsilon) + 1] \quad (2)$$

where the factor $(1-R_c)$ is included because a cube band with another cube neighbour will not provide nuclei and C_c is a constant.

Nucleation from grain boundary regions (pre-existing high-angle boundaries) has also been included in the model. These grains will show a weak deformation texture, but will to a large extent be of random orientations [8], as more and other slip systems are active in the periphery of a grain during deformation (resulting in a randomisation of the subgrain orientations at the grain boundaries). In analogy with Eq. (2) the density of grain boundary nuclei becomes:

$$N_{GB} = 2C_{GB} (\delta_{GB}/\bar{D})(1 - R_C)S_{GB}^* [\exp(\varepsilon) + \exp(-\varepsilon) + 1] \quad (3)$$

where δ_{GB} is the subgrain size and C_{GB} is a constant.

The next step becomes to calculate the recrystallisation kinetics. The growth rate of a recrystallised grain is defined by the grain boundary mobility, M , and the effective driving pressure through the relationship $G=M(P_D-P_Z)$ where the mobility is assumed to be orientation-independent ($M=[M_0/RT]\exp[-U/RT]$, where an activation energy of $U=200\text{kJ/mol}$ was chosen based on annealing tests). The driving pressure is determined by the energy stored in the subgrain boundaries:

$$P_D = \alpha\gamma_{SB}/\delta \quad (4)$$

where γ_{SB} is the average sub-boundary energy which can be calculated by the Read-Shockley relation, δ is the average subgrain size and α is a geometric constant of the order of 3. During steady state hot deformation the following relationship between the subgrain size and the Zener-Hollomon parameter has been reported [9]:

$$\frac{1}{\delta} = A \ln Z - B \quad (5)$$

with $A=0.165 \cdot 10^6 \text{m}^{-1}$ and $B=3.87 \cdot 10^6 \text{m}^{-1}$ for a hot deformed AlMgMn alloy. The recrystallisation kinetics is calculated by applying the standard assumptions of site saturation and a random distribution of nucleation sites, i.e. the following transformation kinetics law is obtained:

$$X(t) = 1 - \exp\left[-\frac{4}{3}\pi N_{TOT}(G \cdot t)^3\right] \quad (6)$$

where $X(t)$ is the fraction recrystallised after an annealing time t . When the fraction recrystallised is determined the grain size in the recrystallised regions can be calculated as $D=(X/N_{TOT})^{1/3}$, while the fractions of the three recrystallisation texture components are given as $f_i=N_i/N_{TOT}$. The situation is rather plain in cases of single pass deformation, but the model has also been extended to a multipass situation aimed at modelling a complete industrial hot rolling schedule. The calculation of the total number of nucleation sites (N_{TOT}) is not trivial in the complex situation of partly recrystallised subregions during multipass deformation. In a material of grain size D_0 and an initial cube fraction R_C^0 the total number of nucleation sites after the 1st deformation pass becomes $N_{TOT}=N_C+N_{GB}+N_{PSN}$

(see Eqs. 1-3). After the 2nd rolling pass the situation becomes more complex. Due to partial recrystallisation with a transformed fraction X_1 after the 1st pass, the material now consists of two subregions, X_1 and $(1-X_1)$, which must be treated separately. The number of sites after the second pass is then given by $N_{TOT}^2 = (1-X_1)(N_C^{1,2} + N_{GB}^{1,2}) + X_1(N_{GB}^2 + N_C^2) + N_{PSN}$, where $N_C^{1,2}$ is to be understood as cube regions which survived the first pass without recrystallisation, while N_C^2 originates from cube areas that recrystallised after the first pass. The calculation of particle sites is independent of the former recrystallisation history since the density of PSN-nuclei is only dependent on the driving pressure achieved in the previous pass (see Eq. 1). The total number of nucleation sites after the n -th pass can be formulated as:

$$N_{TOT}^n = N_{PSN}^n + X_{n-1}(N_C^n + N_{GB}^n) + \sum_{i=0}^{n-2} X_i \cdot \left[\prod_{j=i+1}^{n-1} (1 - X_j) \right] \cdot \left[N_C^{i+1, \dots, n} + N_{GB}^{i+1, \dots, n} \right] \quad (7)$$

where $N_C^{i+1, \dots, n}$ is the number of cube sites originating from cube areas that have survived the passes (i+1) to (n-1) without recrystallising while N_C^n is due to cubes that recrystallised in the pass prior to the n -th. The expression for $N_C^{i+1, \dots, n}$ is of the form:

$$N_C^{i+1, \dots, n} = f \left(D_i, \bar{\delta}_C^n, S_{C,n}^*, \sum_{j=i}^n \varepsilon_j, R_j^i \right) \quad (8)$$

where the function f is specified in Eq. (2). Grain boundary sites are to be treated in a similar manner with the use of Eq. (3).

Table 1: Rolling schedule and measured parameters for Gränges hot rolling mill (h: sample thickness, Z: Zener-Hollomon parameter, Δt : inter-pass time after given deformation pass, X: fraction recrystallised, D: grain size after inter-pass time and f_c : recrystallised cube fraction).

Pass	h-in [mm]	h-out [mm]	Strain	Rate [1/s]	Temp. [C]	Z [1/s]	Δt [s]	X [%]	D [μm]	f_c [%]
1	310	280	0.10	2.1	550	1.7×10^{10}	8	-	-	-
2	280	255	0.09	2.2	545	2.0×10^{10}	9	-	-	-
3	255	230	0.10	2.4	540	2.5×10^{10}	10	-	-	-
4	230	205	0.12	2.6	535	3.2×10^{10}	10	-	-	-
5	205	180	0.13	2.9	528	4.3×10^{10}	10	-	-	-
6	180	155	0.15	3.4	521	6.2×10^{10}	11	-	-	-
7	155	130	0.18	3.9	514	8.8×10^{10}	12	-	-	-
8	130	105	0.21	4.6	507	1.3×10^{11}	14	-	-	-
9	105	80	0.27	5.8	500	2.0×10^{11}	17	5	25	-
10	80	60	0.29	6.7	485	3.8×10^{11}	20	<3%	-	-
11	60	40	0.41	9.0	465	9.9×10^{11}	27	10	25	-
12	40	25	0.47	11.6	450	2.2×10^{12}	40	20	55	-
13	25	17	0.39	13.4	425	6.3×10^{12}	57	10	20	-
14	17	11.5	0.39	16.3	400	2.1×10^{13}	155	15	40	15
T1	11.5	5	0.83	12.0	400	1.5×10^{13}	3	0	0	-
T2	5	2.3	0.78	40.5	340	7.9×10^{14}	anneal	100	25	12

3. EXPERIMENTAL

The model has been applied to industrial hot rolling by a reversible mill in combination with a 2-stand tandem mill at Gränges. The rolling of the 310mm thick slabs included 14 passes in a reversible mill and two tandem passes, taking the material down to a thickness of 2.3mm. No samples were taken from the first 8 passes, but the structure of the 9th pass showed that no recrystallisation has taken place in the first 8 passes (<3% in each pass). Deformation conditions and measured quantities are given in Table 1. Notice that the listed deformation conditions are best estimates, which have been averaged over each deformation pass. All measured data are from the centre section, but the measured quantities are incomplete and rather inaccurate due to measuring difficulties. The investigated material was a 3004-type alloy of chemical composition Al-0.5Fe-0.2Si-1.3Mg-1.0Mn-0.17Cu-0.03Zn-0.019Ti (wt%). It had an initial grain size of 100 μm and was homogenised for 6h at 570°C. Particle size distributions were measured in the as-homogenised condition and transformed to 3D distributions by a Schwartz-Saltikov treatment, giving the following parameters: $N_0=1.0\cdot 10^{16}\text{m}^{-3}$ and $L=1.3\cdot 10^6\text{m}^{-1}$. The material also contained a density of 5.7 μm^{-2} small dispersoids (of typical sizes 0.1 μm) which contribute with a retarding Zener drag.

4. MODEL PREDICTIONS AND COMPARISON WITH EXPERIMENTAL RESULTS

The model contains some model parameters that have to be determined by tuning the model to the experimental data. Here, the model was tuned to a recrystallised fraction of 17% after the 12th pass, a recrystallised cube fraction of 15% after the 14th pass and a grain size of 25 μm after batch-annealing after the final pass. This gave the following model constants: $C_C=0.04$, $C_{\text{PSN}}=0.05$ and $C_{\text{GB}}=0.01$. Two different approaches were taken with respect to Zener drag from dispersoids: (i) no Zener drag and (ii) a constant Zener drag of $P_z=1\times 10^5\text{J/m}^3$. In both cases the pre-exponential of the mobility-expression, M_0 , was adjusted to give 17% recrystallisation after the 12th pass. A value of $M_0=1.95\times 10^6$ and $M_0=4\times 10^6$ were used for cases without and with Zener drag, respectively.

Model predictions are compared to measured data for the case without Zener drag in Fig. 1. The figure shows the fraction recrystallised, recrystallised cube fraction and recrystallised grain size. Notice that the cube fraction corresponds to a fully recrystallised condition, while the grain size is the actual grain size in a partly recrystallised condition (just before the material enters the next rolling pass). It is seen that the model gives a too high fraction recrystallised for the passes prior to the 12th, and a too low fraction for the subsequent passes. The cube fractions are reasonable compared to experimental data, while the predicted grain size is generally smaller than the measured values. In summary, it must be said that the model without a Zener drag does not give a good description of the real situation.

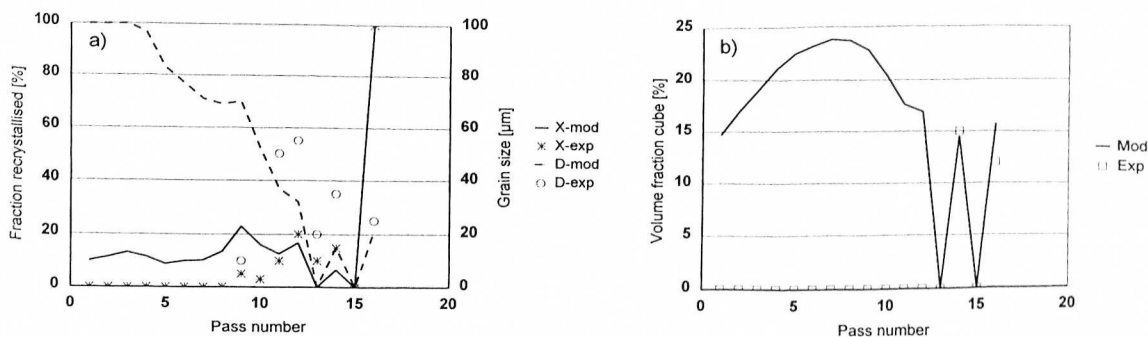


Fig. 1: Fraction recrystallised (X), cube fraction (in a fully recrystallised condition) and grain size (D) as a function of pass number for the case where a Zener drag is not included in the model.

Figure 2 shows the predictions where a Zener drag is included in the model. The constant Zener drag has the largest effect for the first passes where the driving pressure for recrystallisation is small, and little effect for the final rolling passes where the driving pressure is much larger than the Zener drag. It is seen that the model predictions are considerably improved, and the fractions recrystallised are very well predicted for all passes. The experimental data for the recrystallised cube fraction are insufficient for a test of the model. Again, the modelled grain size is slightly lower than the measured (although the agreement is better than for the case without a Zener drag). This is believed to be partly due to difficulties measuring small, partly recrystallised and very elongated grains by optical microscopy, and partly due to their anisotropic growth. The grains became very elongated, which is believed to be due to an inhomogeneous distribution of precipitates. Such effects are not taken into account in the model.

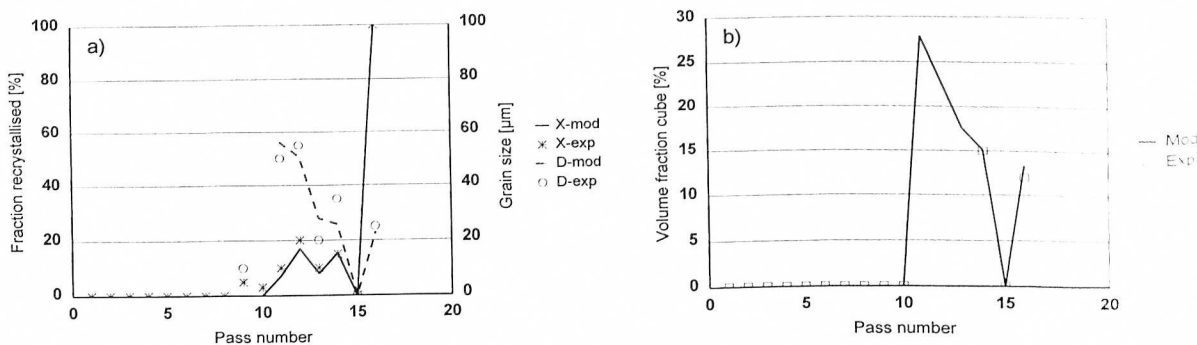


Fig. 2: Fraction recrystallised (X), cube fraction (in a fully recrystallised condition) and grain size (D) as a function of pass number for the case where a Zener drag is included in the model.

5. CONCLUDING REMARKS

The modelling of the hot rolling of a 3004 alloy has shown that a retarding Zener drag from dispersoids must be included in order to obtain a good prediction power. The model predictions are in good agreement with experimental data, which confirms the basic assumptions and physical mechanisms in the model. However, the available experimental quantities are not sufficient for a true test of the model. Samples and measurements from more passes will be aimed at in future, also for alloys that give higher fractions of recrystallisation between the deformation passes.

REFERENCES

- Sellars C.M., *Mat. Sc. Tech.*, **6**, pp. 1072-1081, (1990)
- Reyes G.C., Beynon J.H., in "Hot Deformation of Aluminium Alloys", (eds. T.G. Langdon, H.D. Merchant, J.G. Morris, M.A. Zaidi), pp. 491-508, The Min., Met. and Mat. Soc., (1991)
- H. E. Vatne, T. Furu, R. Ørsund and E. Nes, *Acta Metall.*, **44**, 4463-4473, (1996).
- H. E. Vatne, K. Marthinsen, R. Ørsund and E. Nes, *Met. Trans. A*, **27A**, 4133-4144, (1996)
- Humphreys F.J., *Acta Metall.*, **25**, pp. 1323-1344, (1977)
- H. E. Vatne, T. Furu and E. Nes, *Materials Science and Technology*, **12**, 201-210, (1996)
- H. E. Vatne, R. Shahani and E. Nes, *Acta Metallurgica et Materialia*, **44**, 4447-4461, (1996)
- Engler O., *Mat. Sc. Tech.*, **12**, 859, (1996)
- Castro-Fernandez F.R., Sellars C.M., Whitemann J.A., *Mat. Sc. Tech.*, **6**, 453, (1990)